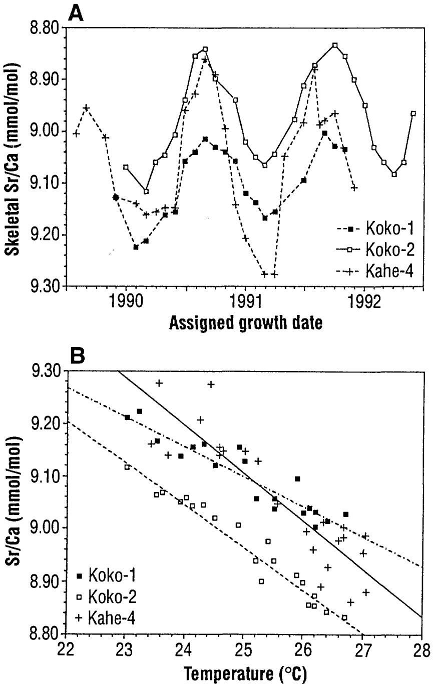

Fig. 2. (**A**) Seasonal variations in skeletal Sr/Ca of three Hawaiian *Porites lobata* specimens from Koko Head, Oahu (Koko-1 and Koko-2) and Kahe Point, Oahu (Kahe-4). (**B**) Sr/Ca-temperature relation established for each of the *Porites lobata* specimens on the basis of the SST record at each sampling site. The regression lines are $[Sr/Ca]_{Koko\text{-}1} = 10.52 - 0.0569T$ (r = 0.97), $[Sr/Ca]_{Koko\text{-}2} = 10.96 - 0.0795T$ (r = 0.99), and $[Sr/Ca]_{Kahe\text{-}4} = 11.36 - 0.0904T$ (r = 0.95).

bolic activity of the coral is subject not only to temperature but to changes in factors such as light intensity, sea level, turbidity, and nutrient supply (*17*). Environmental stress resulting from a change in any of these factors may produce slower extension and calcification rates (*17*), which would imply enriched skeletal Sr/Ca values or apparently colder LGM temperatures. If suboptimal growth conditions prevailed during glacial-interglacial transitions and resulted in enhanced skeletal Sr/Ca uptake, the Sr/Ca thermometer may overestimate the real SST change. Our results suggest that unless these effects are understood to an extent that would allow a retrospective assessment of their magnitude in fossil corals, coralline Sr/Ca values cannot be considered an absolute proxy of past SST variations.

REFERENCES AND NOTES

1. C. M. Clapperton, *Quat. Sci. Rev.* **9**, 299 (1990); M. A. Bush *et al.*, *Quat. Res.* **34**, 251 (1990).
2. CLIMAP Project Members, *Geol. Soc. Am. Mar. Chart Ser. MC-36* (1981).
3. T. J. Crowley, *Nature* **371**, 664 (1994); D. Rind and D. Peteet, *Quat. Res.* **24**, 1 (1985); C. Emiliani and D. F. Ericson, *Geochem. Soc. Spec. Publ. 3* (1991), p. 223; M. T. Chen, J. Imbrie, W. L. Prell, *Eos* **74**, 32 (1993); J. Hansen *et al.*, in *Climate Processes and Climate Sensitivity*, J. Hansen and T. Takahashi, Eds. (American Geophysical Union, Washington, DC, 1984), pp. 130–145; Intergovernmental Panel on Climate Change, *Climate Change: The IPCC Scientific Assessment* (Cambridge Univ. Press, Cambridge, 1990).
4. J. W. Beck *et al.*, *Science* **257**, 644 (1992).
5. T. P. Guilderson, R. G. Fairbanks, J. L. Rubenstone, *ibid.* **263**, 663 (1994).
6. S. de Villiers, thesis, University of Washington (1994).
7. J. N. Weber, *Geochim. Cosmochim. Acta* **37**, 2173 (1973); G. Thompson and H. D. Livingstone, *Limnol. Oceanogr.* **16**, 786 (1971); R. C. Harriss and C. C. Almy, *Bull. Mar. Sci. Gulf Caribb.* **14**, 418 (1964); T. S. Cross and B. W. Cross, *J. Sediment. Petrol.* **53**, 587 (1983); R. C. Schneider and S. V. Smith, *Mar. Biol.* **66**, 121 (1982).
8. L. S. Land *et al.*, *Mar. Biol.* **33,** 221 (1975); T. J. Goreau, *Proc. R. Soc. London* **196**, 291 (1977); ______ and N. I. Goreau, *Biol. Bull.* **117**, 239 (1959). $\delta^{18}O$ is the normalized deviation, in parts per thousand, of the sample $^{18}O/^{16}O$ relative to standard mean ocean water.
9. S. de Villiers *et al.*, *Geochim. Cosmochim. Acta* **58**, 197 (1994).
10. The Sr/Ca ratio was determined by isotope dilution on a VG Sector solid-source mass spectrometer (Sr in static mode, Ca by peak jumping). An exponential mass fractionation law (*11*) was used for $^{84}Sr/^{86}Sr$ and $^{44}Ca/^{42}Ca$, assuming natural abundances of $^{84}Sr/^{88}Sr = 0.1194$ (*12*) and $^{42}Ca/^{44}Ca = 0.31221$ (*13*). Repeat analysis of an internal coral standard over a 2-year period yielded an external measurement precision of 0.1% (1σ, $n = 15$). $\delta^{18}O$ analyses were carried out on the same subsamples, as described (*14*). Small sample sizes resulted in an average error associated with replicate analysis of 0.17% along the 6 mm/year transect and 0.08% along the 12 mm/year transect.
11. W. A. Russel *et al.*, *Geochim. Cosmochim. Acta* **42**, 1075 (1978).
12. A. O. Nier, *Phys. Rev.* **54**, 275 (1938).
13. B. D. Marshall, thesis, University of California, Los Angeles (1984).
14. M. K. Gagan *et al.*, *Earth Planet. Sci. Lett.* **121**, 549 (1994).
15. T. A. McConnaughey, *Geochim. Cosmochim. Acta* **53**, 151 (1989).
16. S. V. Smith, R. W. Buddemeier, R. C. Redalje, J. E. Houck, *Science* **204**, 404 (1979).
17. C. D. Clausen and A. A. Roth, *Mar. Biol.* **33**, 93 (1975); R. C. Highsmith, *J. Exp. Mar. Biol. Ecol.* **37**, 105 (1979); R. P. M. Bak, *Proc. 2nd Int. Coral Reef Symp.* **2**, 229 (1974); R. W. Buddemeier, *ibid.*, p. 259; R. E. Dodge and G. W. Brass, *Bull. Mar. Sci.* **34**, 280 (1984); R. E. Dodge, R. C. Aller, J. Thomson, *Nature* **247**, 574 (1974); E. H. Gladfelter and R. K. Monohan, *Proc. 3rd Int. Coral Reef Symp.* **2**, 389 (1977).
18. We thank B. Hales, R. Sonnerup, and others for discussions of this work. Supported by National Oceanographic and Atmospheric Administration grant NA36GP0209 (G. T. Shen).

17 March 1995; accepted 19 June 1995

Temperature Measurements of Shock-Compressed Liquid Hydrogen: Implications for the Interior of Jupiter

W. J. Nellis,* M. Ross, N. C. Holmes

Shock temperatures of hydrogen up to 5200 kelvin were measured optically at pressures up to 83 gigapascals (830 kilobars). At highest pressures, the measured temperatures are substantially lower than predicted. These lower temperatures are caused by a continuous dissociative phase transition above 20 gigapascals. Because hydrogen is in thermal equilibrium in shock-compression experiments, the theory derived from the shock data can be applied to Jupiter. The planet's molecular envelope is cooler and has much less temperature variation than previously believed. The continuous dissociative phase transition suggests that there is no sharp boundary between Jupiter's molecular mantle and its metallic core. A possible convectively quiescent boundary layer might induce an additional layer in the molecular region, as has been predicted.

Jupiter, the largest planet in the solar system, has long been of considerable interest to astronomers. This planet is composed primarily of hydrogen with about 10 atomic % helium; the interior is at high pressures (P) and high temperatures (T) because of the large mass and low thermal conductivity (*1*). For example, the boundary between the molecular hydrogen mantle and the metallic hydrogen core is estimated to be 300 GPa (3 Mbar) and 10,000 K at 0.77 of Jupiter's radius (*2*). Pressures and temperatures at the center range up to 4 TPa and 20,000 K. Conditions in planetary interiors are calculated from theoretical models that are consistent with the observed mass, radius, rotational rate, gravitational moments, and surface chemical composition. Density (ρ) distributions are calculated from the gravitational moments, which are very sensitive to the equation of state at very high pressures and temperatures (*3*). Because the internal temperatures are well above the calculated melting curve of hydrogen, Jupiter is in the fluid phase (*4*); the interior is assumed to be fully convective and adiabatic and to obey an isentropic equation of state. Here, we report shock temperature measurements of liquid hydrogen and their implications for the nature of the interior of Jupiter.

Shock-compression measurements of the equations of state of hydrogen and helium

---

Lawrence Livermore National Laboratory, University of California, Institute of Geophysics and Planetary Physics and H Division, Livermore, CA 94550, USA.

*To whom correspondence should be addressed.

(5–8) achieve thermodynamic states that are representative of those found in planetary interiors (4). Hugoniot data are P-ρ measurements along the Hugoniot or shock-compression curve. Temperatures must be calculated from theoretical models, which use intermolecular potentials fitted to the P-ρ shock-compression data, or measured in separate experiments such as reported here. Earlier models of jovian isentropes were calculated from equations of state that were based on Hugoniot P-ρ data. All the recent modeling shows that H_2 begins to dissociate above 20 GPa and 4500 K and that the dissociation process is continuous to higher pressures and temperatures. The same models indicate that at room temperature hydrogen becomes monatomic at pressures of 300 to 500 GPa, which occur deep within Jupiter. Our temperature data show that molecular dissociation occurs continuously above 20 GPa.

Temperature measurements are more sensitive to dissociation than are P-ρ data, especially near the onset of dissociation. Dissociation causes the absorption of a few electron volts per molecule, which results in a considerable drop in temperature when the dissociation fraction is more than a few percent (9). However, detection of the pressure change caused by dissociation in doubly shocked hydrogen requires higher accuracy than can be achieved by the P-ρ method. Over the past few years, we have developed sophisticated optical methods for the measurement of shock temperatures (10). These temperature data provide an important constraint on the equation of state.

We generated high pressures and temperatures in liquid deuterium samples with the use of a two-stage light-gas gun that accelerated a tantalum or aluminum impactor toward the sample holder (5, 11); the deuterium temperatures were measured optically (Fig. 1) (12). The impactor reached velocities up to 7 km/s, and the resulting shock temperatures ranged from 2820 K at 12.0 GPa to 5210 K at 82.8 GPa. Temperatures measured for pairs of first shocks and second shocks in deuterium are plotted versus molar density in Fig. 2. The solid lines connect the first-shock and second-shock temperatures measured in each experiment, described in detail elsewhere (13).

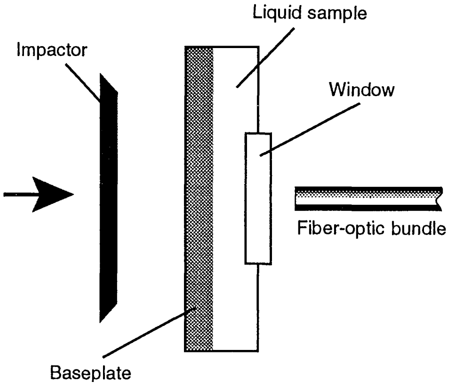

Fig. 1. Schematic of the experiments. The impactor is accelerated to velocities up to 7 km/s and generates a strong shock wave on impact with the baseplate [see (12)].

The first-shock temperatures at pressures up to 22 GPa agree well with predictions that neglect dissociation (7, 13). However, the second-shock temperatures at highest pressures (~80 GPa), densities, and temperatures are substantially lower than predicted for a purely molecular fluid. These lower temperatures are caused by the partial and continuous dissociation of hydrogen into monatomic hydrogen, as observed in nitrogen (14). Because the hydrogen theories of Ross *et al.* (RRY) (7) and Saumon and Chabrier (SC) (15) considerably overestimate these shock temperatures, we developed a model to agree with these measured hydrogen temperatures. Our model introduces a softer equation of state for the dissociated species relative to the molecular species, which lowers the dissociation energy and allows for the absorption of more kinetic energy than is predicted without dissociation. Temperatures calculated with our model (16) are in excellent agreement with the measured shock temperatures in Fig. 2.

Hydrogen in shock experiments is in thermal equilibrium. The time of one vibrational period of a free H_2 molecule is 0.8×10^{-14} s; this value changes by only a few percent at high pressures (17). At the density (0.25 mol/cm^3) and temperature (5000 K) associated with our highest pressure (83 GPa), the time between molecular collisions is $\sim 4 \times 10^{-14}$ s. Thus, within our time resolution of 3×10^{-9} s, hydrogen undergoes 10^5 collisions and vibrations, which is more than sufficient to achieve thermal equilibrium. Our results are thus independent of whether we make our measurements in 100 ns or in a billion years. For this reason, the theoretical equation of state derived from our shock data is applicable to the interior of Jupiter.

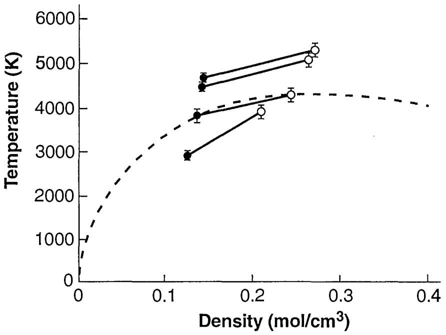

Fig. 2. Measured first-shock (solid circles) and second-shock (open circles) temperatures of deuterium. Solid lines join pairs of first-shock and second-shock temperatures measured in each experiment (Fig. 1). The highest first-shock pressure is 22.6 GPa, and the highest second-shock pressure is 82.8 GPa. The first-shock temperatures are in good agreement with predictions based on the molecular phase (7). The highest second-shock temperatures are lower than predicted because H_2 is undergoing partial dissociation at highest densities and pressures. The present model was developed to agree with all the shock-temperature data. The dashed curve is the hydrogen isentrope calculated with the present model from the surface conditions of Jupiter (165 K and 1 bar). Because the calculated isentrope passes through the region of the shock data, these shock-temperature data probe temperatures and densities in Jupiter.

The present model was used to calculate the isentrope of hydrogen starting from the surface conditions of Jupiter, 165 K and 1 bar (Fig. 2). This isentrope was calculated up to 200 GPa, which requires an extrapolation from our maximum experimental density of 0.26 mol/cm^3 up to 0.4 mol/cm^3. At 200 GPa the calculated dissociation fraction is 15%, which is a modest perturbation of the molecular equation of state. The measured first- and second-shock temperatures are in the same region as this calculated isentrope, which illustrates that our shock-temperature data probe the pressures and temperatures in Jupiter (4). The maximum in $T(\rho)$ in Fig. 2 might be an artifact because the temperature decrease at higher densities is small and the model has been extrapolated to higher densities than were achieved in our experiments. Also, in Jupiter the ~10 atomic % helium causes temperature to increase monotonically with density and pressure because helium has no internal energy absorption mechanism, such as dissociation or electronic excitation, at the temperatures involved.

The present isentrope of hydrogen is plotted as T versus P in Fig. 3, together with the RRY result for pure H_2 and the SC result, which includes some calculated dissociation. Our model in Fig. 3 shows that the continuous dissociation of H_2 keeps the isentropic temperatures relatively constant near 4000 K over

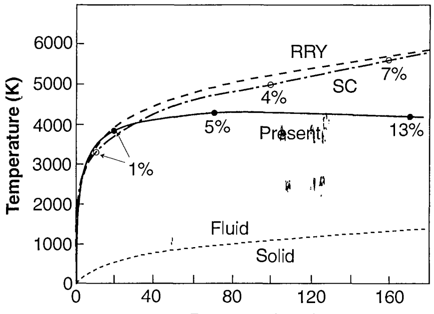

Fig. 3. Isentropes of hydrogen (calculated from 165 K and 1 bar) plotted as temperature versus pressure for the present model, the RRY result (7), and the SC result (15). Dissociation fractions calculated with the present and SC models are indicated. A calculated melting curve (4) is also shown.

a wide range of pressures (and thus depth) from 30 to 180 GPa. Our model also predicts that at 180 GPa, dissociation of 13% of the H_2 yields an isentropic temperature of hydrogen that is about 25% lower than the RRY and SC results at highest pressures. Thus, the jovian isentrope in the molecular layer is cooler and has substantially smaller temperature variation than previously thought.

The continuous dissociative phase transition in hydrogen suggests that no sharp boundary exists at what is now called the core-mantle boundary. That is, as H_2 dissociates continuously to the monatomic phase and eventually metallizes, there probably is no sharp discontinuity in the relative composition of the molecular and metallic phases nor in density.

Figure 3 indicates that the spatial gradient in the equilibrium temperature distribution is small. In addition to this equilibrium temperature distribution, there is also a small nonequilibrium "excess" temperature distribution caused by gravitational energy deposited during formation of the planet. This "excess" energy is slowly radiated by Jupiter, and the resulting slow cooling causes the radius of Jupiter (7×10^{10} mm) to decrease by ~1 mm/year (*18*). The radial gradient of this excess temperature drives convection and is a relatively large fraction of the total thermal gradient because the equilibrium thermal gradient is small in the phase-transition region (Fig. 3). Thus, our results provide strong evidence for the assumption that the molecular layer is fully convective. As the dominant heat conduction mechanism, convection causes the temperature distribution to approach the isentropic distribution (*18*). Convection also generates the planetary magnetic field by dynamo action (*19*). Magnetic effects are important in the molecular layer (*20*), and a portion of the magnetic field might be generated there.

The ρ-*P* isentropes corresponding to the *T*-*P* curves in Fig. 3 are plotted in Fig. 4. The ρ-*P* curve is much less affected than the *T*-*P* curve by the change in the equation of state, and ρ increases monotonically with *P*. At 180 GPa, the density calculated by the present model is only 8% higher than the SC result, with the RRY result halfway between. Our results have a weak effect on the calculated density variation and thus exert a relatively weak effect on modeling the density distribution to match flyby data of the gravitational field.

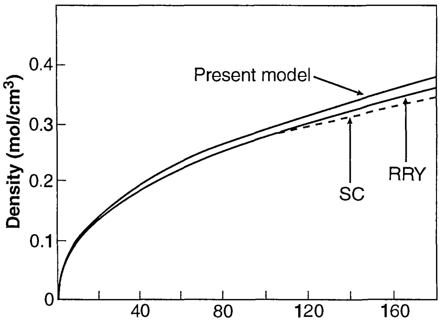

Fig. 4. Plot of density versus pressure for the three isentropes in Fig. 3.

The possible existence of a maximum in temperature (Fig. 3) depends on the actual details of this curve and the presence of He and planetary ices and rocks (*2*). However, if a maximum in *T*(*P*) were to exist, such a temperature distribution might have important effects on convection. If, for example, convection were to depend only on the radial temperature gradient, then this gradient would change sign on either side of the maximum in *T*(*P*). In this case, convection would be upward toward the surface on one side and downward toward the center on the other side of the maximum. As a result, a quiescent boundary layer might be expected at depths corresponding to pressures of 30 to 180 GPa. A quiescent boundary layer over a long period of time might facilitate separation of ice and rock and cause an abrupt density change. A boundary has been proposed at 42 GPa on the basis of an analysis of gravitational field data (*2*). At greater depths, the pressure becomes sufficient to completely dissociate and metallize hydrogen, and a further increase in depth causes the temperature to increase monotonically with pressure. Hence, there might be a local minimum in temperature near the radius of what is now called the molecular mantle–metallic core boundary. In this case, convection would be driven toward the temperature minimum from both larger and smaller radii, causing a convectively turbulent region.

Recently, the first observations of global free oscillations of Jupiter have been reported (*21*). Their frequency is ~20% less than expected for current models. This frequency is determined by the velocity of sound and thus depends on the equation of state. If these oscillations are, in fact, seismic oscillations, then sound velocities ~20% less than currently calculated over the entire planet must be explained (*21, 22*).

The velocity of sound *c* is given by $c^2 = (\partial P/\partial \rho)_S$, where *S* is entropy. All the *P*-ρ isentropes in Fig. 4 have nearly the same slopes; hence, the value of *c* calculated with our model is only a few percent less than was previously calculated. Although the change is in the appropriate direction, it is too small to explain the ~20% reduction required in *c*. However, our calculations to 200 GPa probe only the outermost 15 to 20% of the radius of Jupiter. Increasing the percentage of He or the ices would reduce *c* but would also result in a larger density than Jupiter is known to have. Because hydrogen is metallic in the inner ~75% of the radius of Jupiter, any relatively large correction of *c* must occur in the metallic phase, at still higher pressures and temperatures than reported here. Neither laboratory experiments nor theoretical calculations have been performed in this extremely complex region. A proper evaluation of the reported seismic data awaits a recalculation of Jupiter's internal structure based on an equation of state that includes our temperature data, as well as future measurements and their theoretical analysis in the metallic liquid phase.

REFERENCES AND NOTES

1. W. B. Hubbard, *Science* **214**, 145 (1981); D. J. Stevenson, *Annu. Rev. Earth Planet. Sci.* **10**, 257 (1982); V. N. Zharkov and V. P. Trubitsyn, in *Jupiter*, T. Gehrels, Ed. (Univ. of Arizona Press, Tucson, 1976), pp. 135–175.
2. V. N. Zharkov and T. V. Gudkova, in *High-Pressure Research: Application to Earth and Planetary Sciences*, Y. Syono and M. H. Manghnani, Eds. (Terra Scientific, Tokyo, 1992), pp. 393–401.
3. R. Smoluchowski, *Nature* **215**, 691 (1967).
4. M. Ross, H. C. Graboske, W. J. Nellis, *Philos. Trans. R. Soc. London Ser. A* **303**, 303 (1981).
5. W. J. Nellis *et al.*, *J. Chem. Phys.* **79**, 1480 (1983).
6. M. van Thiel *et al.*, *Phys. Rev. Lett.* **31**, 979 (1973); R. D. Dick and G. I. Kerley, *J. Chem. Phys.* **73**, 5264 (1980).
7. M. Ross, F. H. Ree, D. A. Young, *J. Chem. Phys.* **79**, 1487 (1983).
8. W. J. Nellis *et al.*, *Phys. Rev. Lett.* **53**, 1248 (1984).
9. Molecular dissociation at ~80 GPa absorbs an energy of ~2 eV per molecule; 2 eV corresponds to 23,000 K. Thus, a dissociation fraction of 10% causes a temperature decrease of ~2000 K.
10. N. C. Holmes, *Rev. Sci. Instrum.* **66**, 2615 (1995).
11. A. C. Mitchell and W. J. Nellis, *ibid.* **52**, 347 (1981); W. J. Nellis and A. C. Mitchell, *J. Chem. Phys.* **73**, 6137 (1980).
12. The impactor velocity is measured in free flight with pulsed x-radiography. The ρ-*P* states achieved on impact can be determined by the standard shock-impedance matching method, using the measured impactor velocity and the equations of state of the impactor, the Al baseplate, the liquid hydrogen sample, and the window (either Al_2O_3 or LiF). The impact generates a shock wave in the baseplate, which is transmitted into the liquid and then double-shocks off the window. The first shock in the liquid is observed as a sharp rise (a few nanoseconds) to a steady optical emission when the shock from the baseplate breaks into the liquid. The second shock in the liquid is observed as a second sharp increase in optical intensity when the first shock reflects off the window. The emitted thermal radiation is coupled to a six-channel photomultiplier (PMT) array with fiber optics. Each PMT is sensitive to a narrow-wavelength band 20 nm wide. The temperatures and emissivities are obtained by fitting the PMT data to a Planck spectrum. Most specimens were deuterium because deuterium has a higher shock temperature than hydrogen for a given impactor, hence deuterium temperatures are easier to measure. The first-shock temperatures are on the Hugoniot curve by definition. The second-shock temperatures are reflected from various points on the Hugoniot curve. These second-shock points are at known values of *P*, ρ, and *T*, but are not on a simple curve.
13. N. C. Holmes, M. Ross, W. J. Nellis, in preparation.
14. H. B. Radousky, W. J. Nellis, M. Ross, D. C. Hamilton, A. C. Mitchell, *Phys. Rev. Lett.* **57**, 2419 (1986); W. J. Nellis *et al.*, *J. Chem. Phys.* **94**, 2244 (1991); M. Ross, *ibid.* **86**, 7110 (1987).
15. D. Saumon and G. Chabrier, *Phys. Rev. A* **44**, 5122 (1991).
16. Our model for the fluid is appropriate for the molecular phase with ~15% of dissociated molecules. The regime in which hydrogen begins to dissociate is calculated by interpolation between the two phases by means of linear mixing. That is, the free energy of the partially dissociated hydrogen is calculated from

$$F(V,T) = (1 - x)F_{H_2}(V,T) + F_{H\text{-}H}(V,T) + TS_{mix} - (1 - x)D^0$$

where x is the fraction of dissociated molecules and is determined by minimizing the free energy. The dissociation energy of an isolated molecule is D^0, and the mixing entropy term makes a small contribution. The free energy of the molecular phase, F_{H_2}, was determined previously using soft-sphere perturbation theory to find the molecular potential that agrees with available experimental shock and static data. Fully dissociated monatomic hydrogen is approximated as a nearly free-electron metal. The free energy of this monatomic phase, $F_{H\text{-}H}$, combines a density-dependent, nearly free-electron gas, a modified one-component–plasma ion-thermal energy for the fluid, and an adjustable parameter chosen to agree with all our pressure-temperature and pressure-volume data. We also include a density-dependent function chosen to force agreement at 0 K with ab initio calculations [T. W. Barbee and M. L. Cohen, *Phys. Rev. B* **44**, 11563 (1991)] of the free energy of the body-centered-cubic–phase metal. Thus, the phenomenological model we have adopted builds in the correct limiting behavior for the low-density molecular fluid and high-density monatomic fluid and interpolates smoothly between them.

17. H.-K. Mao and R. J. Hemley, *Rev. Mod. Phys.* **66**, 671 (1994).
18. W. B. Hubbard, *Rev. Geophys. Space Phys.* **18**, 1 (1980).
19. D. J. Stevenson, *Rep. Prog. Phys.* **46**, 555 (1983).
20. R. L. Kirk and D. J. Stevenson, *Astrophys. J.* **316**, 836 (1987).
21. B. Mosser, *Astron. Astrophys.* **251**, 356 (1991).
22. T. S. Duffy, W. L. Vos, C.-S. Zha, R. J. Hemley, H.-K. Mao, *Science* **263**, 1590 (1994).

23. This work was performed under the auspices of the U.S. Department of Energy by the Lawrence Livermore National Laboratory under contract W-7405-ENG-48, with support from the National Aeronautics and Space Administration under grant W 16.180. We thank W. B. Hubbard, D. Saumon, R. J. Hemley, and T. S. Duffy for helpful discussions and T. W. Barbee III for making available unpublished calculations. We thank E. See, J. Crawford, S. Weaver, J. Ulrech, P. McCandless, and R. Silva for assistance in performing these experiments and R. Kays of the Lockheed Missile and Space Company for providing the liquid hydrogen coolant.

31 October 1994; accepted 21 March 1995

Ab Initio Calculation of the Sound Velocity of Dense Hydrogen: Implications for Models of Jupiter

Ali Alavi,* Michele Parrinello, Daan Frenkel

First-principles molecular dynamics simulations were used to calculate the sound velocity of dense hydrogen, and the results were compared with extrapolations of experimental data that currently conflict with either astrophysical models or data obtained from recent global oscillation measurements of Jupiter. Excellent agreement with the extrapolated experimental data was obtained. These results strongly support the notion that the existing models for the jovian interior need to be revised.

Although hydrogen is the simplest of all elements, its properties at high pressures (in the 100-GPa regime) and temperatures (several thousand kelvin) are not well understood. Hydrogen in such physical regimes occurs in abundance in astrophysical bodies such as stars and the giant planets, and thus its properties are of fundamental importance in understanding the physical properties of these bodies. A number of recent experimental and observational breakthroughs may lead to a much better understanding of the properties of hydrogen at these conditions. In particular, Duffy *et al.* (*1*) have measured the sound velocity of dense hydrogen up to pressures of 24 GPa. These measurements were preceded by observations of global oscillations of Jupiter (*2*), from which the planet's "equidistance" has been inferred. The equidistance is the inverse of twice the time it takes for a ray to travel from the planet's center to the surface. In the context of a model for the pressure profile of Jupiter (*3*), this equidistance can be used to obtain an estimate of the sound velocity of hydrogen under the conditions prevailing in the interior of the planet (*1*).

The global oscillation data, combined with a reliable interior model, may provide a convenient way to probe the interesting intermediate temperature regime in which the electron gas is partially degenerate. However, the sound velocities that have been obtained in this way are in substantial disagreement with the measured sound velocities (*1*). At present, the source of disagreement is not clear. To make meaningful comparisons, researchers have extrapolated experimental data (by means of fitting the data to empirical potentials) from 25 to 300 GPa, but this procedure is fraught with uncertainty because in this high-pressure regime hydrogen is expected to undergo a variety of transitions (both first-order and continuous), including a molecular-to-atomic transition (*3*) and a metal-insulator transition. Empirical potentials for H_2, fitted to lower density data, tend to overestimate the repulsive wall of the molecules (*1*). The result is an underestimate of the compressibility of dense hydrogen or, equivalently, an overestimate of the sound velocity. Indeed, the extrapolated "low-pressure" experimental data predict sound velocities in dense hydrogen that are much greater than those inferred from the global oscillation data. However, it cannot be concluded that the extrapolation procedure to estimate the high-pressure sound velocity is in error; the assignment of the global oscillation spectra in (*2*) has been controversial, and the results of the data analysis depend strongly on the choice of the model for the interior of Jupiter. Thus, the apparent disagreement between the jovian global oscillation data and the extrapolated terrestrial results may also signal the need for a revision of the existing models of Jupiter (*1*, *2*). A completely independent measurement of the sound velocity in dense, hot hydrogen would help to clarify these issues. Here, we present ab initio calculations of the sound velocity of hydrogen and compare our results with the above findings.

The prediction of sound velocities over such a broad range of pressures presents a formidable theoretical problem for a number of reasons. First, in this pressure regime the nature of the effective interaction between the protons changes from a completely molecular state to an increasingly dissociated one. A parameter-free model that can consistently describe hydrogen throughout this regime necessitates a proper quantum mechanical treatment of the electrons. In addition, the thermal fluctuations of fluid hydrogen must be properly sampled, which requires a statistical treatment of the protons, and, furthermore, dynamical information is necessary to compute sound velocities. An approach that combines quantum and statistical mechanics is the method of ab initio molecular dynamics (Car-Parrinello method) (*4*), which has recently been successfully applied to the hydrogen plasma (*5*).

The method we used is different in one basic respect from the usual Car-Parrinello method, namely, that it is based on finite temperature density functional theory, as developed in (*6*), rather than ground state (T = 0) density functional theory; this enabled us to check the effect of electronic temperature on the approach to the metallic phase. In our calculations two approximations remain, namely the electronic exchange-correlation functional, which we treat in the local density approximation (LDA) (*7*), and the neglect of the zero-point motion (ZPM) of the protons.

A. Alavi, Department of Chemistry, University of Cambridge, Lensfield Road, Cambridge CB2 1EW, UK, and Trinity College, Cambridge CB2 1TQ, UK.
M. Parrinello, Max-Planck-Institut für Festkörperforschung, Heisenbergstrasse 1, 70569 Stuttgart, Germany.
D. Frenkel, Fundamenteel Onderzoek der Materie (FOM) Institute for Atomic and Molecular Physics, Kruislaan 407, 1098 SJ Amsterdam, Netherlands.

*Present address (from 1 October 1995): School of Mathematics and Physics, Queen's University, Belfast BT7 1NN, Northern Ireland, UK.